Spatial distribution of geomorphic changes after an extreme flash-flood compared with hydrological and sediment connectivity

Adolfo Calvo-Cases[1], Jorge Gago[2,3], Maurici Ruiz-Pérez[3,4,5], Julián García-Comendador[3,4], Josep Fortesa[3,4], Jaume Company[3,4], Beatriz Nácher-Rodríguez[6], Francisco J. Vallés-Morán[6], Joan Estrany[3,4]

[1]Inter-University Institute for Local Development (IIDL) Department of Geography, University of Valencia, Av. Blasco Ibáñez 28, 46010, Valencia, Spain

[2]Biology of plants under Mediterranean Conditions (http://plantmed.uib.es/Ingles/index.html), Department of Biology, University of the Balearic Islands, Carretera de Valldemossa Km 7.5, 07122 Palma, Balearic Islands, Spain

[3]Institute of Agro-Environmental and Water Economy Research –INAGEA, University of the Balearic Islands, Carretera de Valldemossa Km 7.5, 07122, Palma, Balearic Islands, Spain

[4]Mediterranean Ecogeomorphological and Hydrological Connectivity Research Team (http://medhycon.uib.cat), Department of Geography, University of the Balearic Islands, Carretera de Valldemossa Km 7.5, 07122 Palma, Balearic Islands, Spain

[5]Service of GIS and Remote Sensing, University of the Balearic Islands, 07122 Palma, Balearic Islands, Spain

[6]Universitat Politècnica de València, Camí de Vera, s/n, València, 46022, Spain

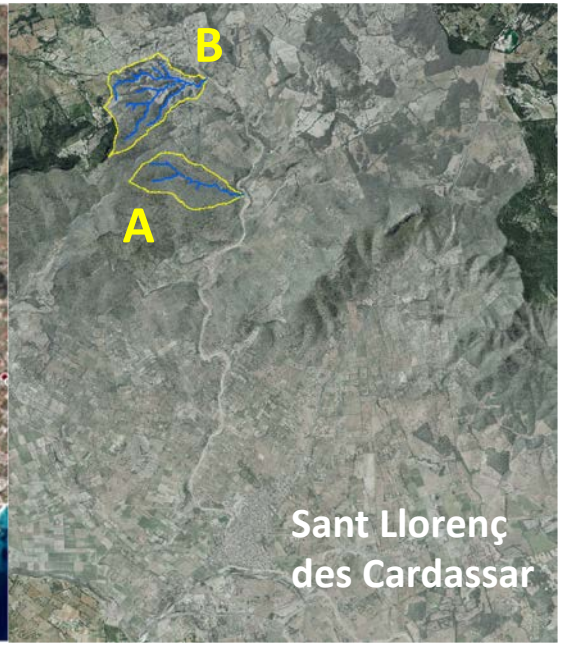

9th October 2018 rainfall evet main characteristics (Estrany et al., 2020)

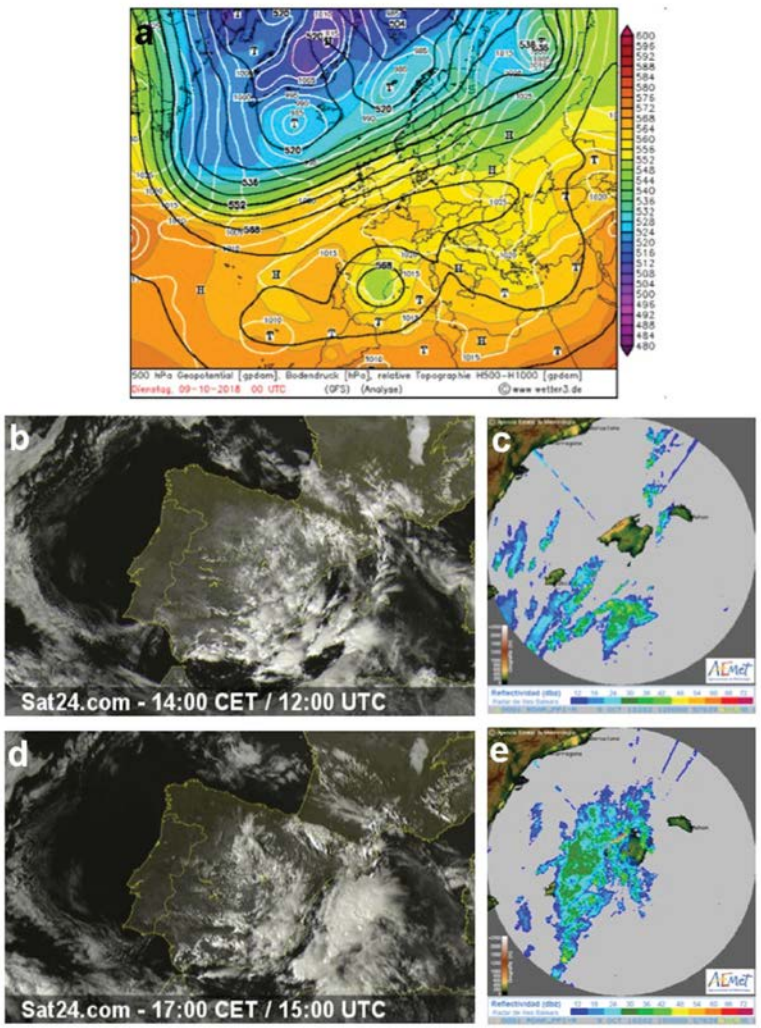

Surface pressure and 500-hPa height analyses at 1200 UTC (http://wetter3.de); i.e. , at the beginning of the event (a). Satellite image at (b) 12.00UTC and (d) 15.00UTC (http://www.sat24.com). EUMETSAT and radar images at the same hours (c and e) (http://www.aemet.es)

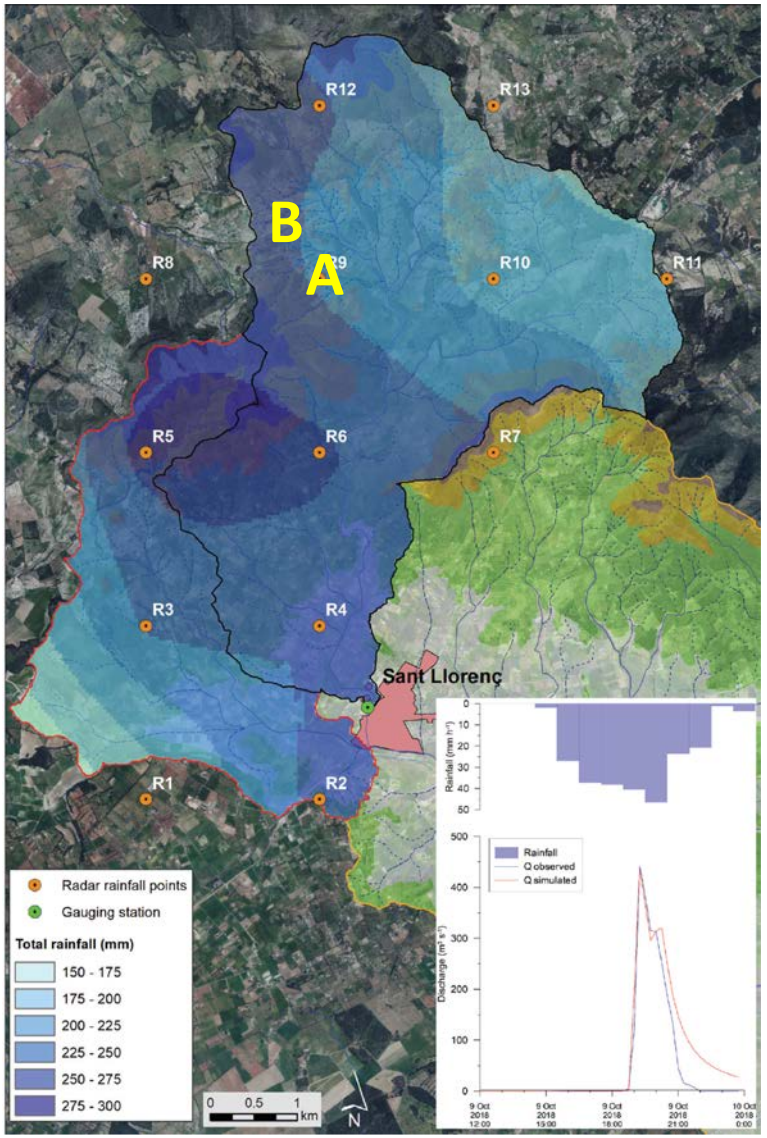

Map of isohyets of the rain storm (10-minute radar images obtained from the web https://opendata.aemet.es/) A-B, Studied catchments.

Main lithology of the studied catchments and distribution of the main made soil conservation structures (SCS).

(C) Cretaceous limestones, clays and marls.
(J) Jurasic limestones and dolomites.
(T) Triasic dolomites

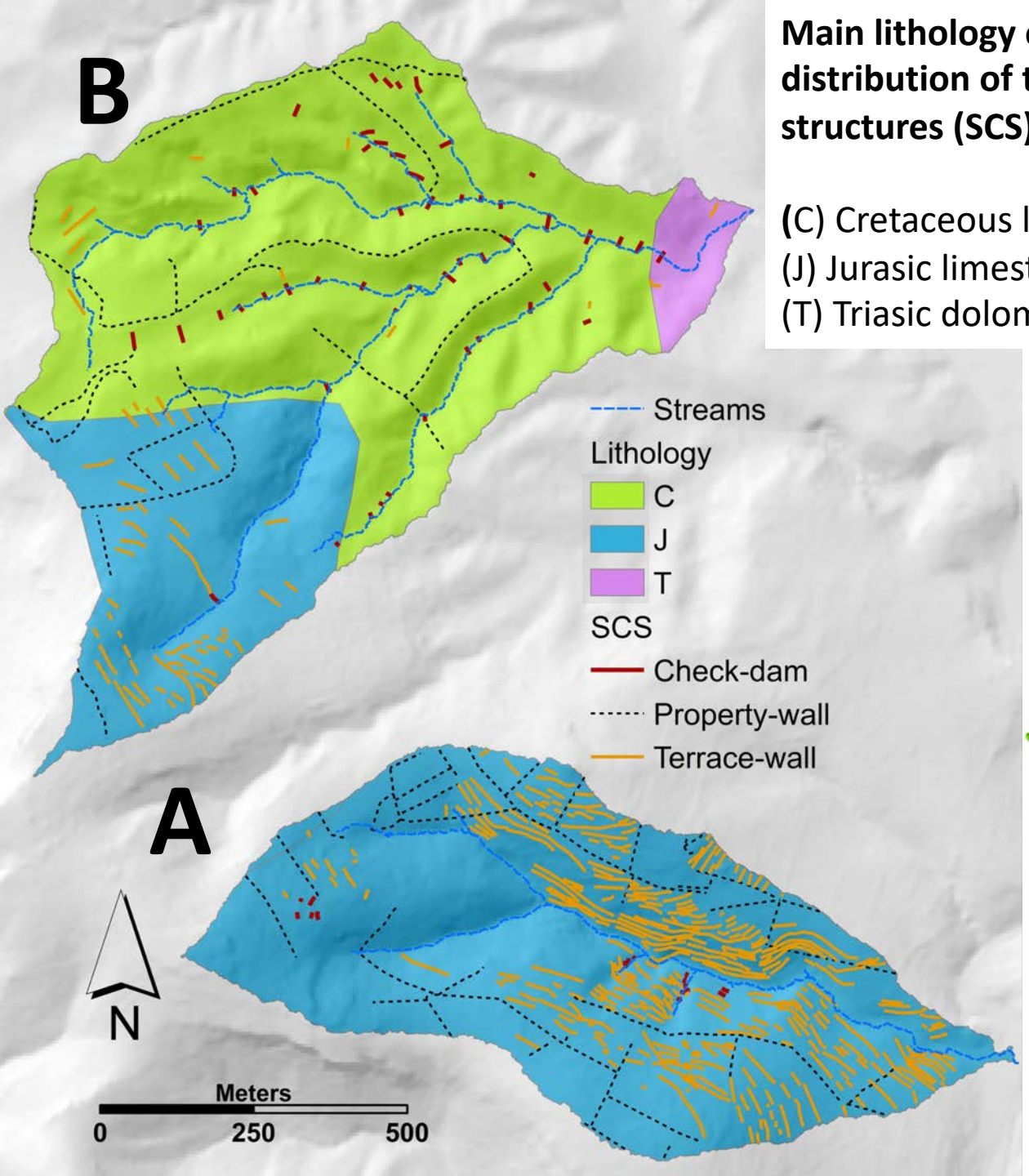

Slope intervals from 1 m LiDAR 2014 DTM.
Average
A = 15.8º B = 19.0º

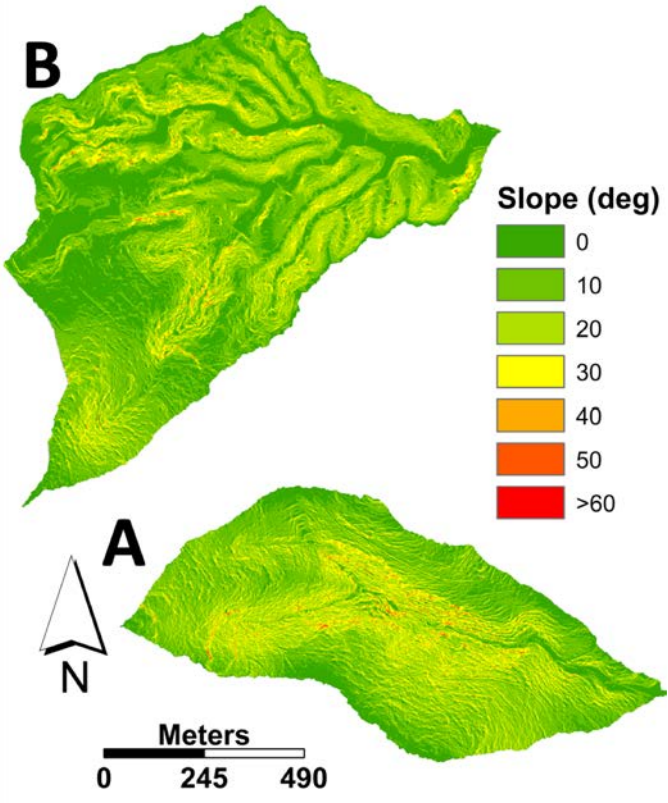

UAVs flight characteristics and processing

Two weeks after the 9th October 2018 event, two UAVs were used to record aerial photographs and build high-resolution digital elevation models. UVA flight characteristics are summarized on the tables and map.

Camera Model	Resolution	Focal Length	Pixel Size
FC6310 (8.8mm)	5472 x 3648	8.8 mm	2.41 x 2.41 µm
ILCE-5000 (16mm)	5456 x 3632	16 mm	4.4 x 4.4 µm

Number of images:	2,515	Camera stations:	2,423
Flying altitude:	143 m	Tie points:	1,977,432
Ground resolution:	3.88 cm/pix	Projections:	7,495,427
Coverage area:	1.22 km²	Reprojection error:	0.797 pix

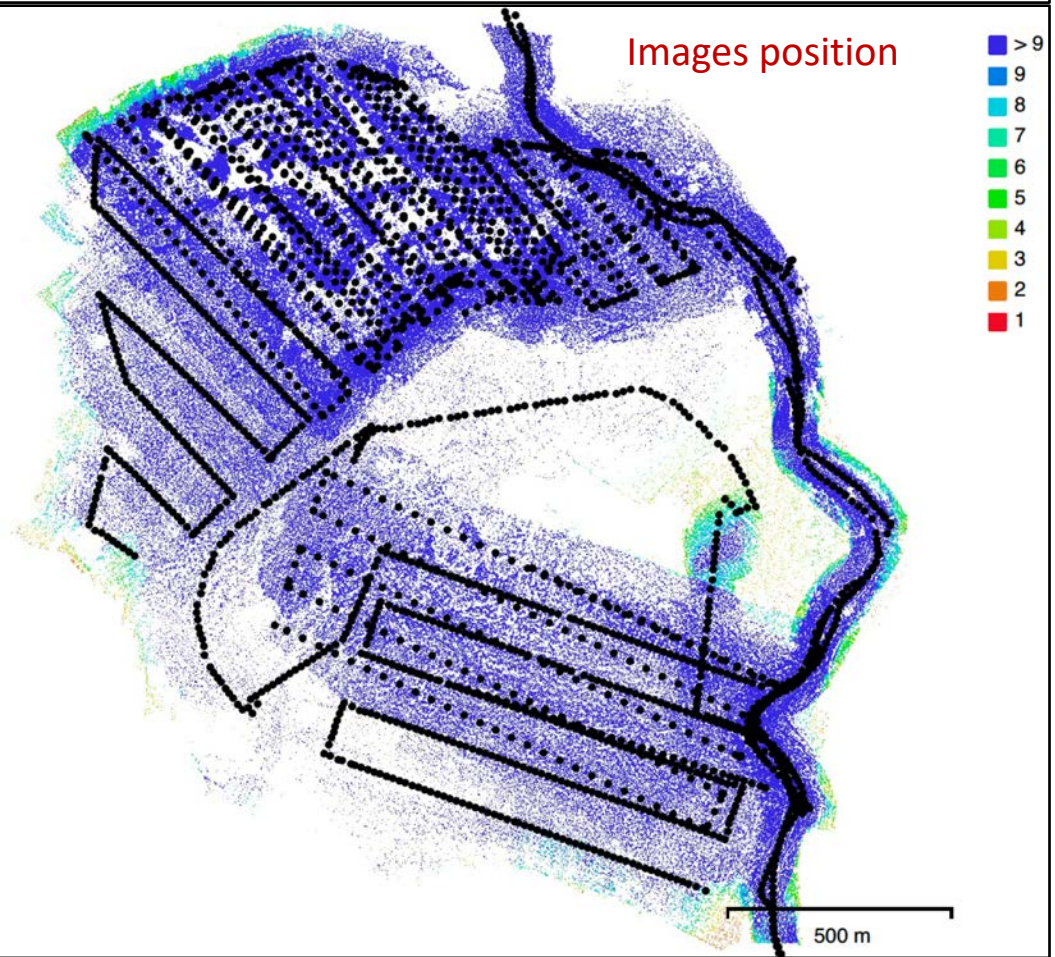

UAV images of the catchments and surroundings were **processed** by means of SfM-MVS procedures using Metashape Pro 1.6 with the following procedure:

1. Convert UAV's GPS coordinates to the coordinate system of GCP (EPSG: 3043)
2. Estimate image quality disabling images with quality below 0.7
3. Align images (quality HIGH, pair preselection: Reference, key point limit: 40,000, tie point limit: 10,000, adaptive camera model fitting: Yes).
4. Import list of GCPs
5. Verifying and linking markers to images
6. Optimize camera alignment
7. Building dense cloud (High)
8. Building DEM (from dense cloud)
9. Building Orthomosaic (based on DEM)

Processing computer: MacBook Pro, i9, 32Gb with GPU-Radeon Pro 560X 4Gb

UAV flight characteristics and processing

Distributed within the two catchments, 83 GCP were marked in the field and coordinates taken with a Leica 1200 differential GPS with the spatial distribution allowed by available tracks.

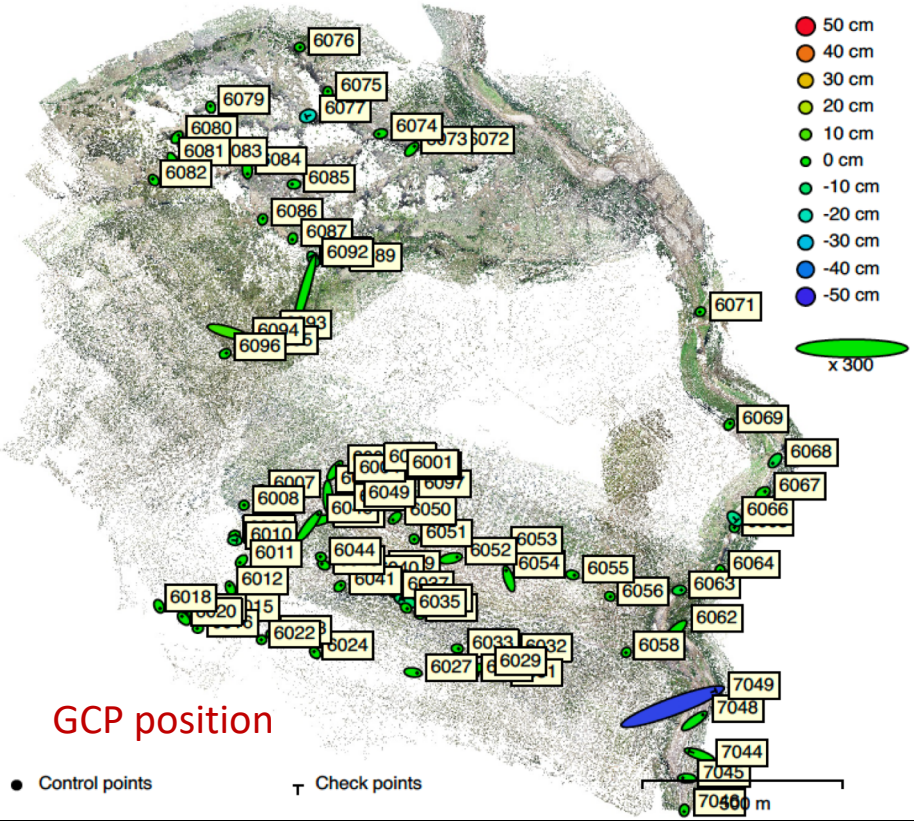

Control points RMSE

Count	X error (cm)	Y error (cm)	Z error (cm)	XY error (cm)	Total (cm)
73	4.52004	5.27666	2.22757	6.94794	7.2963

Check points RMSE

Count	X error (cm)	Y error (cm)	Z error (cm)	XY error (cm)	Total (cm)
10	28.0394	19.839	17.6175	34.3481	38.6027

The GCP with a initial larger RMSE (10 points) where deactivated and considered check points, following the referencing procedure with the remaining 73 points. Resulting provisional DEM and orthoimages have 10 and 5 cm in resolution respectively. Both the orthoimage and the DEM has been proved very useful for identification, mapping and measurement of the erosional forms (see below).

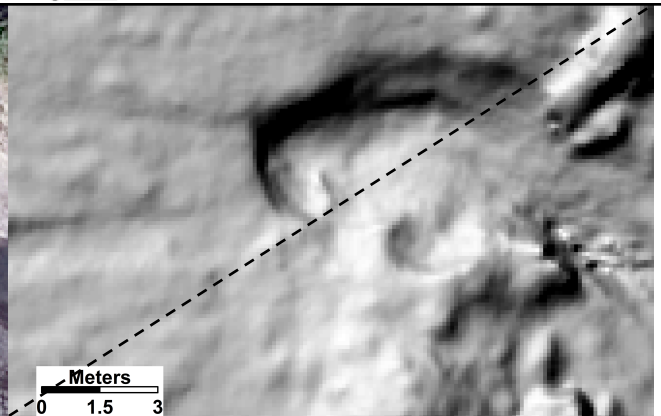

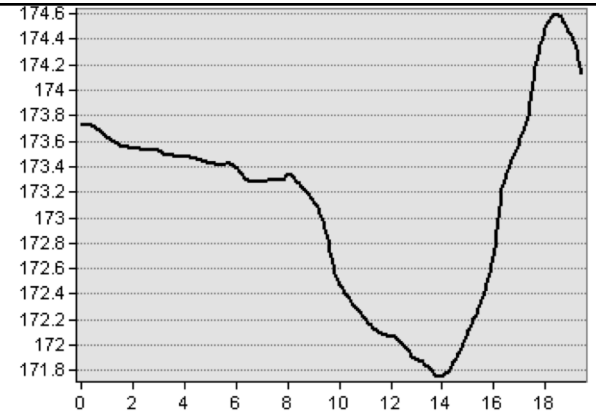

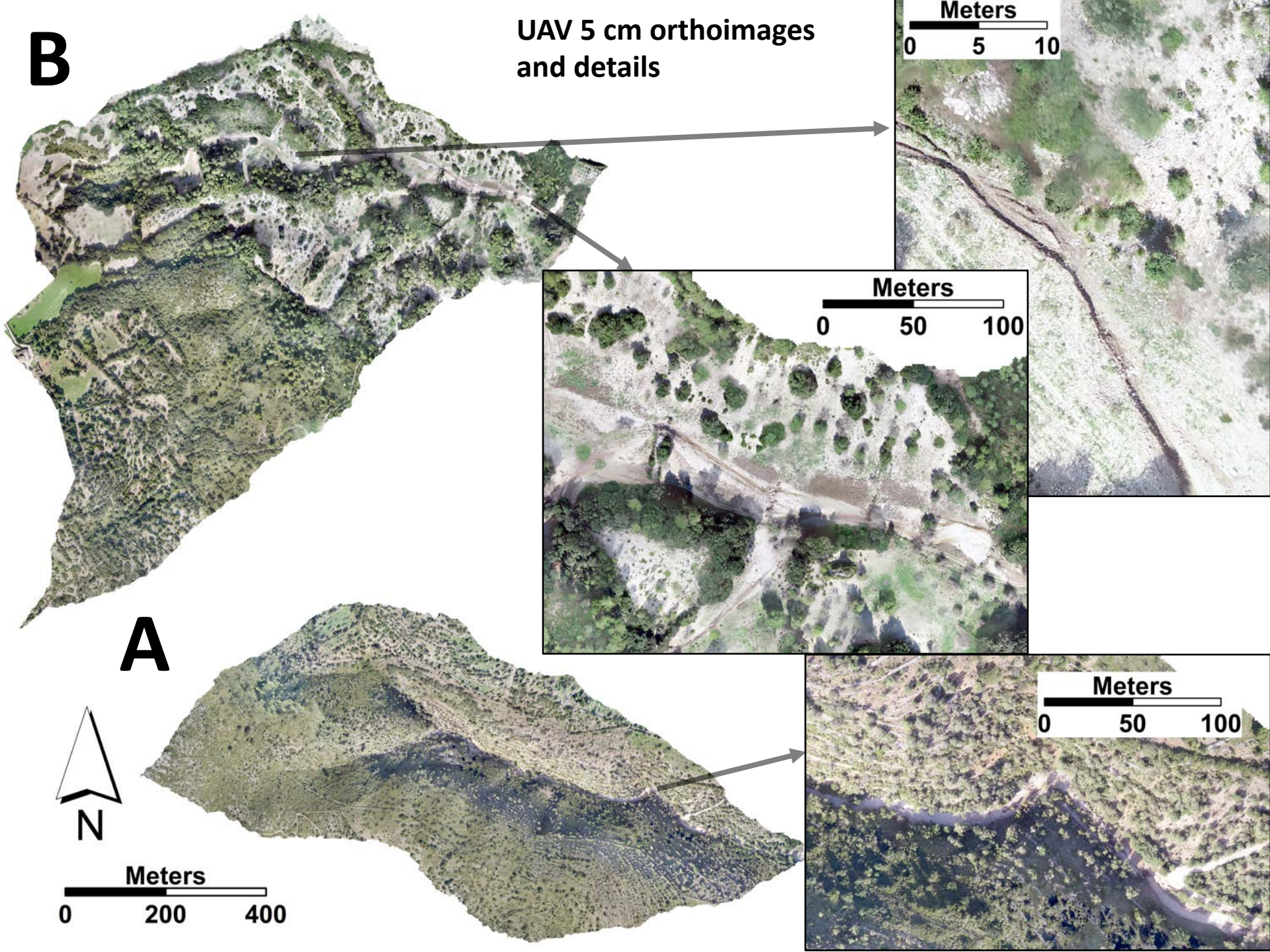
B
UAV 5 cm orthoimages
and details
Meters
0 5 10
Meters
0 50 100
A
N
Meters
0 200 400
Meters
0 50 100

Spatial distribution of the observed response to the rainfall event on the UAV 5 cm resolution orthoimages.

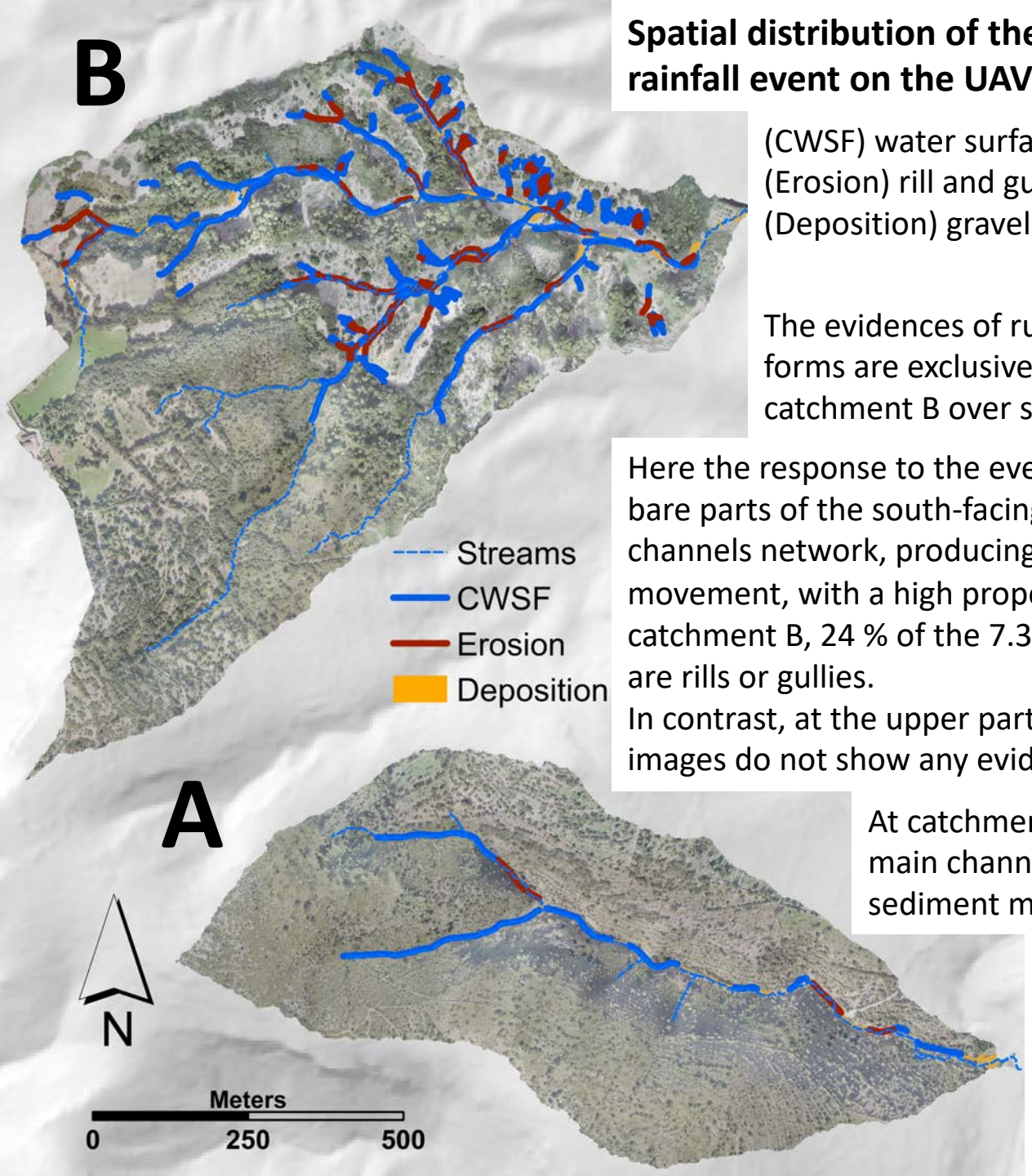

(CWSF) water surface flow evidences.
(Erosion) rill and gully developed during the event.
(Deposition) gravel and fine sedimentation.

The evidences of runoff and, especially dissection forms are exclusively affecting to the parts of catchment B over soft and more erosive material.

Here the response to the event generated mid hillslope rills in bare parts of the south-facing slopes and activated most of the channels network, producing a considerable amount of sediment movement, with a high proportion of gully development. At catchment B, 24 % of the 7.3 Km of lines with runoff evidences are rills or gullies.
In contrast, at the upper part of the B catchment (limestones) the images do not show any evidence of runoff, or erosion.

At catchment A, also on limestones, only the main channel have evidences for runoff and sediment movement.

The limestone areas, have a notable improvement of the matorral cover, in combination with the remains of old agricultural terraces, showing very relevant stability.

DEM of differences (DoD) between the 10 cm DEM obtained from the UAV images and the 1 m LiDAR DTM.

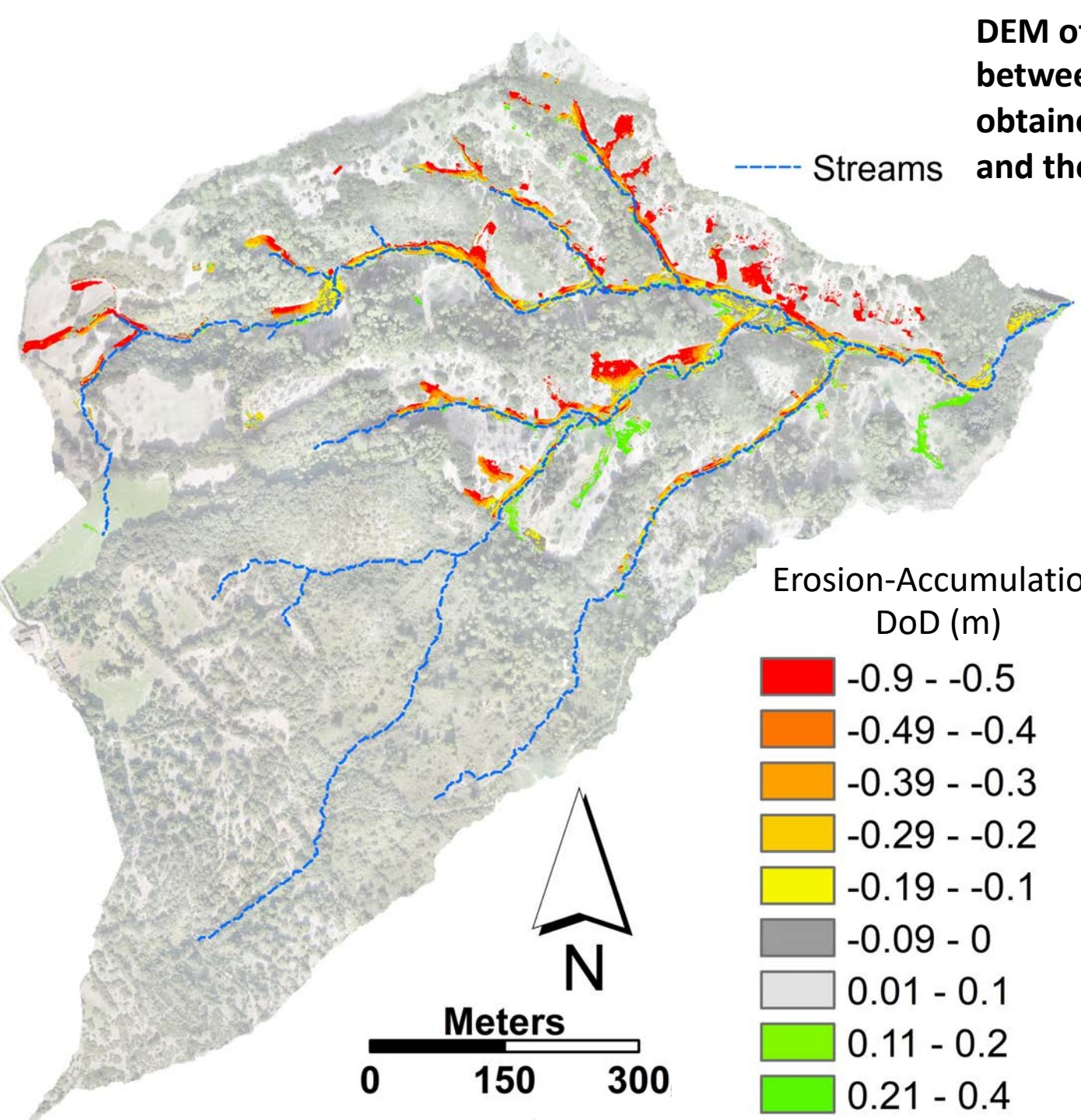

The DoD was made restricted to the areas where erosional and depositional forms were observed, but the differential errors of the two sources (LiDAR DTM and UAV-DEM) increased the erosional figures on south-facing slopes, while create accumulation on the north-facing parts. Alternatively an analysis of the orthoimages and UAV-DEM has been developed.

Some of the cross section extracted from the 10 cm DEM obtained from the UAV images of catchment B. Indications of the assumed original surface and the maximum incision.

As the DoD results were not satisfactory, the eroded parts of catchment B were sampled with 58 cross sections and profile reconstruction was made with the 10 cm DEM. Looking on the orthoimages for the erosion limits the maximum incision was measured in each section.

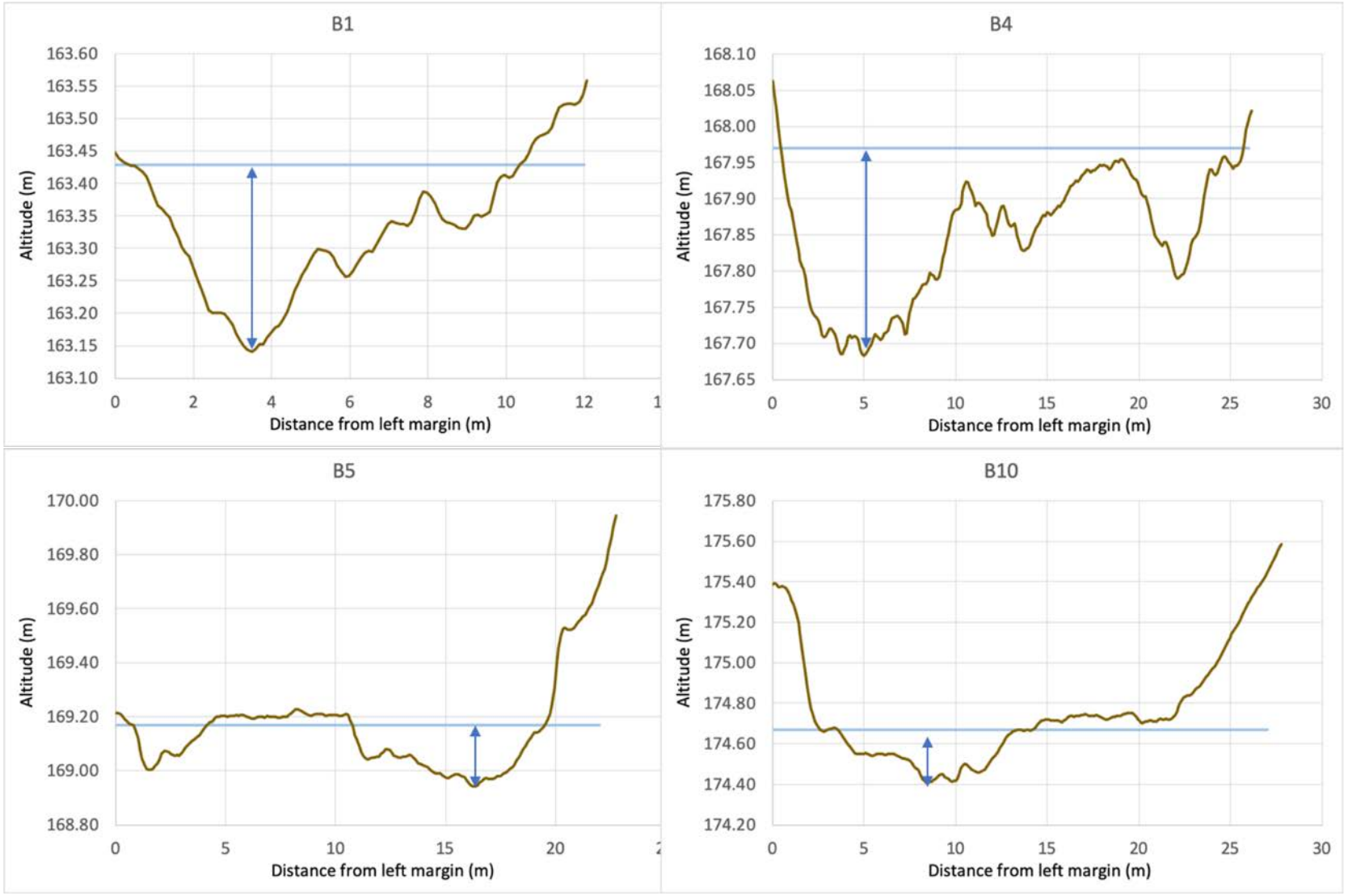

Spatial distribution of the magnitudes of incision and the position of the SCS

The maximum incision measured at each section, reach near 90 cm in depth and half of the sections are over 30 cm (mean 34 cm), over previous surface.

The irregular spatial distribution, show the interferences of the man-made SCS, specially the check-dam style agricultural terraces, that combine the steeps and sediment availability along the talwegs, making variable the sediment concentrations and channel energy. This affects to the certain disparity with the IC values (next slide), showing a poor interdependence, although subgroups are identifiable.

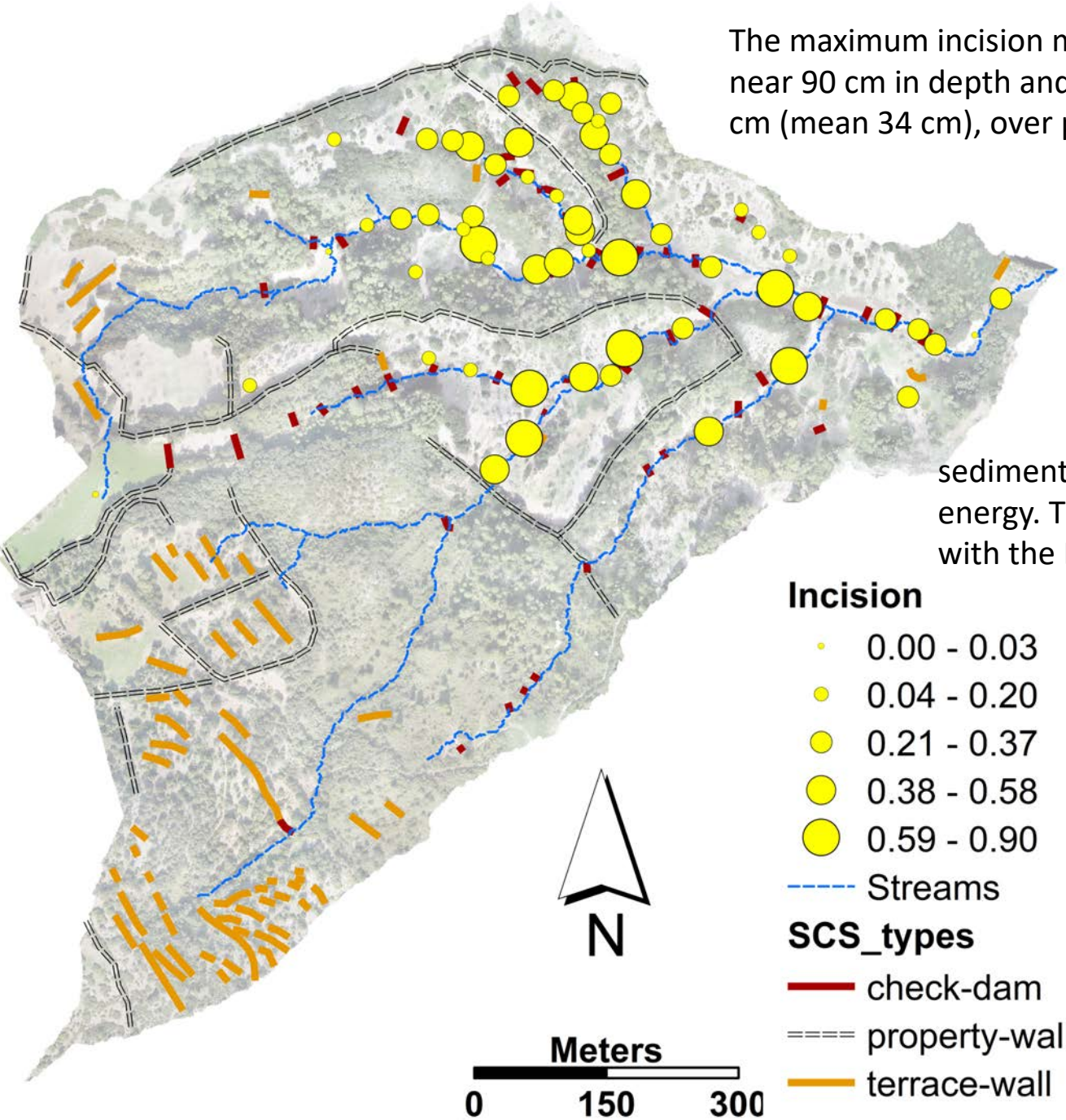

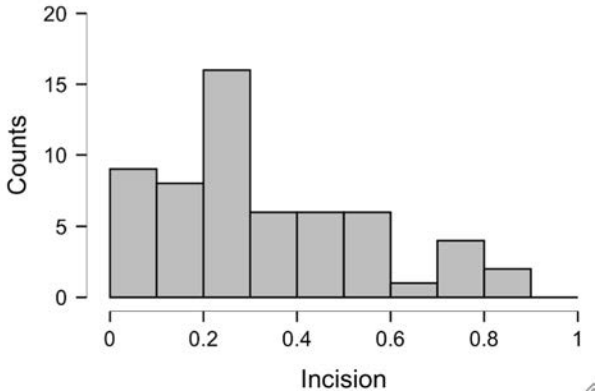

Normalised connectivity index (IC) values for the two catchments.

Extracted from a subset of the Cavalli et al. (2013) IC procedure applied to the whole Begura de Saumà basin to the 1 m LiDAR 2014 DTM.

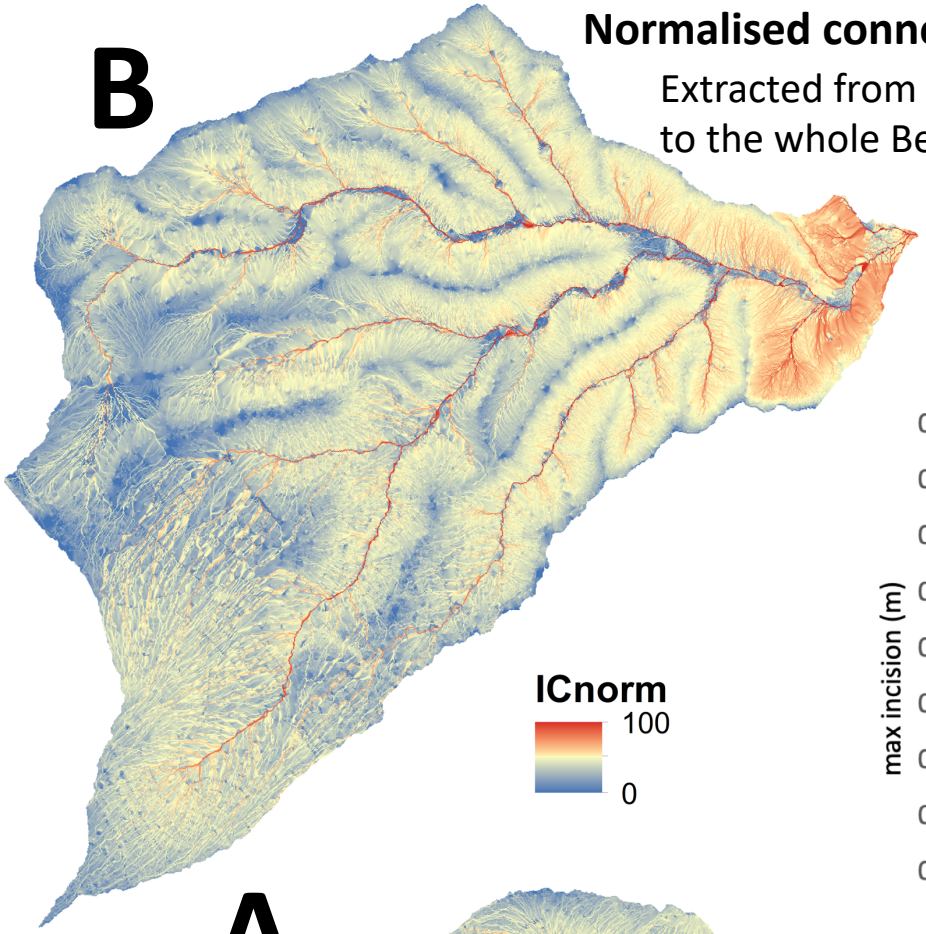

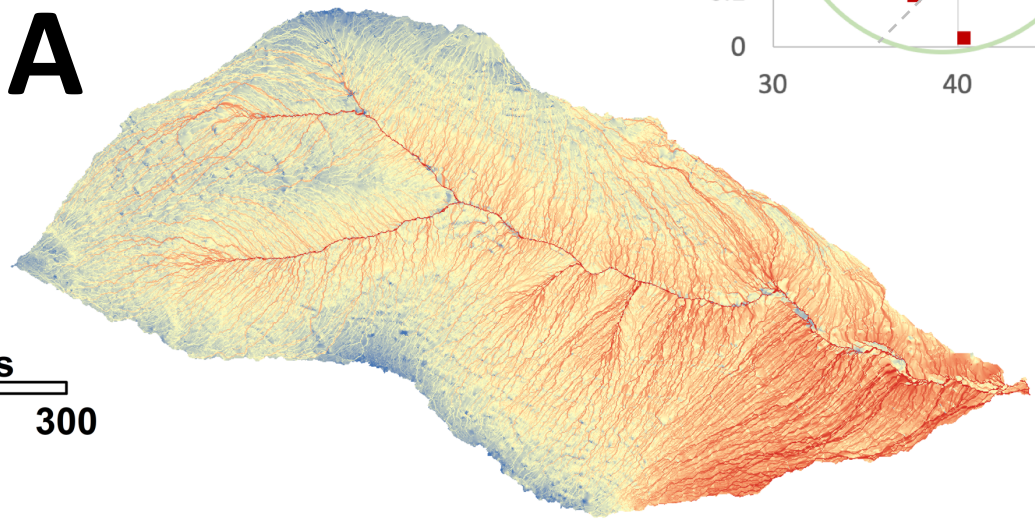

The maximum IC values for for each measured cross section, in catchment B, plotted versus the maximum incision reached, allow to stablish the three main

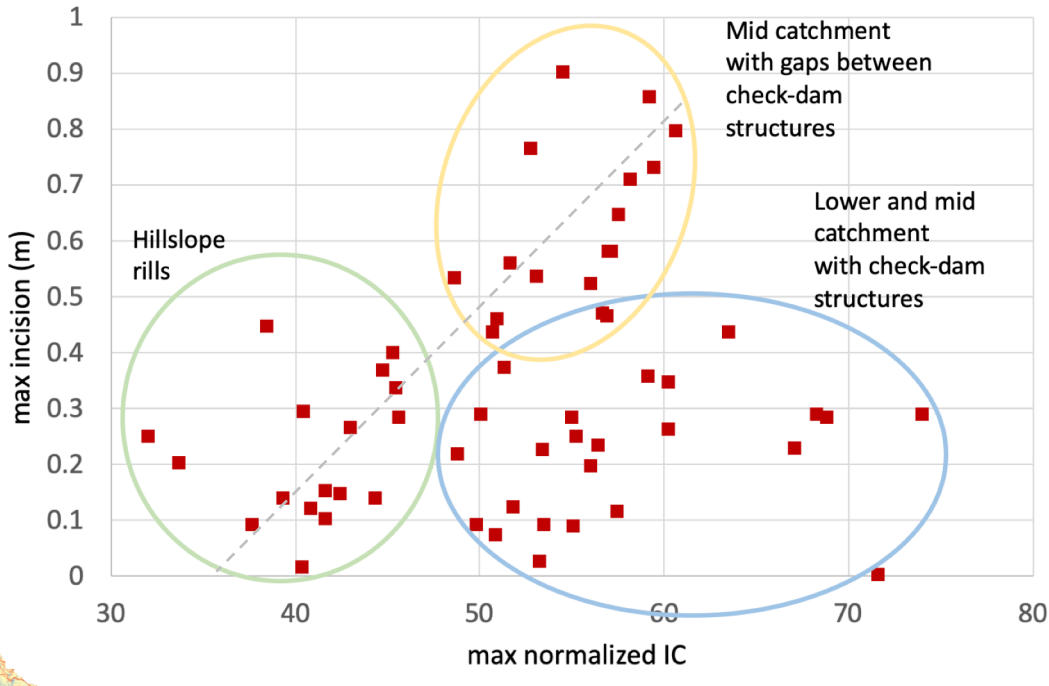

groups visible in the figure, that illustrate how the check-dam terraces can distortion the potential positive trend that draw the set of measurement not directly affected by the artificial structures.